X-ray-absorption near-edge structure spectra for bulk materials: Multiple-scattering analysis versus a phenomenological approach

Peter Kizler
Hamburger Synchrotronstrahlungslabor HASYLAB at Deutsches Elektronen-Synchrotron DESY, Notkestrasse 85, D-2000 Hamburg 52, Germany
(Received 9 December 1991; revised manuscript received 2 July 1992)

X-ray-absorption near-edge structure data evaluations, based on a simple approach to determine bond lengths directly from features of the spectra, have frequently been reported in the literature. This approach is discussed critically taking into account multiple-scattering calculations as well as previously published experimental and theoretical data. All results together demonstrate that this approach can be used for simple molecules, but becomes questionable for condensed-matter analysis.

I. INTRODUCTION

While extended x-ray-absorption fine-structure (EXAFS) spectroscopy has become a widely used tool for structural investigations, the x-ray-absorption near-edge structure (XANES) spectral range is still exploited to a lesser degree. The interpretation of XANES is complicated by multiple-scattering effects as well as by the nonvalidity of the plane-wave-scattering approximation applicable in the EXAFS range. The persisting interest in XANES despite the difficulties arises from several reasons.

(1) For systems with low-Z elements, either the backscattering amplitude or the atomiclike transition matrix elements decay rapidly with increasing k, thereby making conventional EXAFS analysis difficult or impossible in many cases.

(2) Because of the electron multiple-scattering processes occurring in the XANES range, the spectra do not depend only on atomic distances and coordination numbers but also to some extend on higher-order correlation functions[1] like bond angles[2] or the ratio of distances of the x-ray-absorbing atom to its first- and second-shell neighbor atoms.[3]

(3) Finally, it is of general interest to understand the physical processes occuring at the edge.

The variety of physical effects playing a role in understanding the physics of the XANES range is summarized in very comprehensive works[4] and shall not be discussed further here. In the present context the relevant methods for a numerical interpretation of the XANES range of bulk solids are, on the one hand, electronic density-of-states (DOS) calculations, and, on the other hand, single- and multiple-scattering (MS) calculations.

These theoretical methods have already been applied repeatedly and successfully[5] but are still far from being a standard tool for the research. Opposite to the EXAFS data evaluation, a common property of both the DOS and the MS calculations is the lack of a straightforward way from experimental data to structural information. Instead of this, XANES spectra have to be calculated starting from a trial structure. Depending on the agreement between experimental and calculated XANES data, the trial structure may be accepted or rejected. A further disadvantage of the DOS or the MS calculations is that they can be performed easily only for materials consisting of one or two different chemical elements, but materials of practical interest typically are more complex. Finally, the methods require a large amount of computer time, especially for disordered systems. All these disadvantages together have been calling for a more convenient method to derive bond lengths and coordination numbers directly from experimental data.

For simple organic molecules a numerical relationship between the energy position of the XANES peaks and bond lengths was demonstrated[6-8] according to the "kR =const" assumption, set up by Natoli,[9] where k is the photoelectron wave number at energy E_r relative to the average interstitial potential, and R is the distance to the first coordination shell. A similar conclusion had been drawn for metal-O_4 molecules in aqueous solution[10] and in several glasses.[11] Following the spirit of Refs. 6–9 and 11, phenomenological approaches for a straightforward XANES data evaluation have been suggested aiming to interpret the spectra assuming a direct relationship between features in the XANES spectra and bond lengths.[11-13] The authors of Ref. 12 set up a relation $E=150/R^2$, where E is the energy difference of the peculiar XANES feature and a prepeak or the first inflection curve of the XANES data, and R is the referring bond length. An approach using this relation has been applied for several examinations of solids, see, e.g., Ref. 12 and 14–19, however, without proofing the data by a full multiple-scattering calculation.

II. NUMERICAL XANES CALCULATIONS

In order to check the validity of the phenomenological approach, the XANES spectra of two selected examples, which play an important role in the foundation of the approach of Ref. 12, were calculated with full multiple-scattering calculations. The examples are ionic NiO (NaCl structure) and metallic Cu (fcc structure). Con-

vincing full multiple-scattering XANES calculations for these materials have been published previously for NiO,[20] for MgO,[21] which is isostructural to NiO, and for Cu.[22] In the present context it was necessary to compute the spectra again in order to study more details.

For the present work the ICXANES computer code of Vvedensky, Pendry, and Saldin[23] was used. Briefly, the electron transition rate is calculated within the dipole approximation and factorized into an atomic contribution modified by single and multiple scattering of the excited electron by the surrounding atoms. The scattering property of each atom is characterized by the phase shifts δ_l for incident spherical waves of angular momentum l. The phase shifts are calculated by integration of the Schrödinger equation using the program MUFPOT (Ref. 24) assuming a muffin-tin form of the atomic potentials in the bulk, obtained by the superposition of neutral atomic charge densities.[25] The atomic contribution is calculated using a special option of the program MUFPOT employing the transition rule between ground state and excited state.

The phase shifts as well as the atomic contribution and structural data are input for ICXANES, which finally calculates the XANES curves. One advantage of the ICXANES code[23] compared to the previous version by Durham, Pendry, and Hodges[26] is the option to distinguish between intershell and intrashell multiple-scattering paths. Intershell multiple-scattering processes occur in more or less collinear direction between the neighbor shells whereas intrashell multiple-scattering events happen within the shells on triangular or otherwise looped paths.[27] All multiple-scattering processes can even be switched off totally. In this version a curved wave single-scattering calculation is left over, equivalent to sophisticated EXAFS calculation codes.

A. Results for NiO

The top part of Fig. 1 is Fig. 4 out of Ref. 12 with the assumed relation between shells and the XANES features. The dashed line had been calculated as the difference between the experimental data (sold line) and a 5-eV straight-line running average (boxcar smoothing). This procedure simply pulls the feature out of the smoother curve and makes them more visible. The 1s to empty valence transition, typically a prepeak maximum, serves as the zero point of the energy scale.

In the lower part of Fig. 1 the theoretical XANES results for different sizes of the cluster around the x-ray-absorbing atom are displayed togehter with the number of shells used for the calculation. The compositions and distances of the neighbor shells are listed in Table I. The energy scale is relative to the interatomic muffin-tin zero level of the XANES calculation. Due to their differrent definitions, the zero points of the upper and lower scales do not match. For the following discussion only the lower-energy scale related to the XANES calculation will be quoted. The inclusion of even the ninth shell in a distance of 0.66 nm to the x-ray-absorbing atom is justified by the low electron damping in inorganic materials.[28]

For the present calculations the electron damping term was chosen yet smaller than realistic to make the XANES features more pronounced. The XANES calculations yield the densities of states but do not incorporate any knowledge on the Fermi level. Therefore, features at or below the Fermi level appear much more pronounced than they are in the experimental data. To achieve a more realistic result one can convolute the density-of-

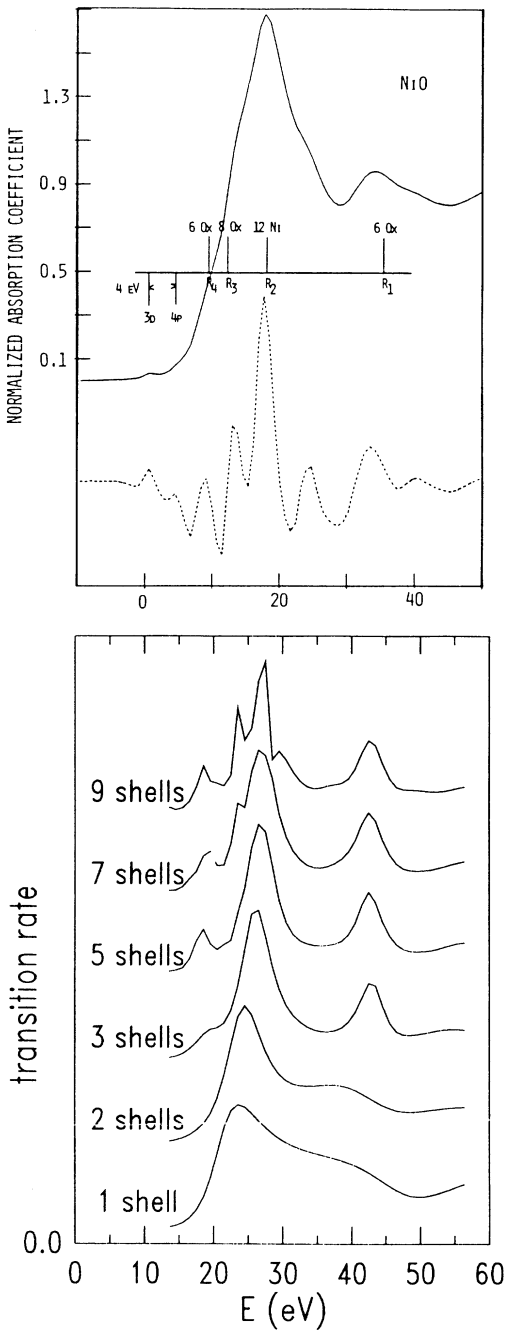

FIG. 1. Top: Experimental XANES data for NIO (Ref. 12) together with the relationship between the XANES features and shells as suggested in Ref. 12. Bottom: Calculated XANES curves for NiO with different cluster sizes. For atomic distances and coordination numbers of the clusters see Table I. Calculations are performed with full multiple scattering.

TABLE I. Shell distances and identities for Ni in NiO (NaCl structure).

Shell No.	Element	N	r (nm)
1	O	6	0.208
2	Ni	12	0.294
3	O	8	0.360
4	Ni	6	0.416
5	O	24	0.465
6	Ni	24	0.509
7	Ni	12	0.588
8	O	30	0.624
9	Ni	24	0.657
10	O	24	0.689

states results with an arctan curve with its inflection point at the Fermi level. In the present context it was more interesting to exhibit sharply the XANES features and their evolution than to reproduce the overall shape, therefore this final step of calculation was not performed. Only those results which differed significantly from the result for the cluster with one shell less were included in the diagram.

The result for the single oxygen shell in octahedral coordination, bottom line, agrees well with experimental data for a NiO_6 cluster.[29] The result for the largest cluster can be compared to the experimental data for NiO (Ref. 12) shown in the top part of Fig. 1. The computated data agree in more details with the experimental data than previously published calculated data[20] do, where the authors did not report the number shells utilized for the calculation. Besides the agreement, one can also state that the large peak above the absorption edge is due to scattering (see also single-scattering results later on) and not to the "historical" $1s$-$4p$ transition. Despite the generally good agreement between experiment and theory, there remains a discrepancy in amplitude as well as a discrepancy between the theoretical and experimental energy positions of the XANES features at the right part of the main peak. It shall be anticipated that, for the case of Cu, see Sec. II B, no such problems were encountered. Therefore, the highly ionic character of NiO seems to be responsible for these problems. Such discrepancies have been observed previously, see, e.g., Ref. 21, and the authors mentioned energy-dependent exchange and correlation effects[30,31] as possible explanations. Also, a mismatch between a true and calculated atomic contribution, caused by the poorer validity of the muffin-tin approximation, should be considered.

Despite these minor problems it can be recognized that the XANES features show up in a manner which is very different from the correlation set up in Ref. 12. For instance, the main peak around 23 eV (on the MS calculation scale), which had been attributed to the first Ni-Ni distance, already exists in the case of only one neighbor shell of oxygen atoms. It only becomes sharper and more structured with increasing the number of shells. An XANES curve is determined by simultaneous backscattering processes from different shells. The way the curves become sharper and more structured with an increasing number of shells reminds one of diffraction patterns obtained from a grating, which also become sharper with an increasing number of lines. A qualitatively equivalent evolution of XANES features related to an increasing cluster size has also been demonstrated using DOS calculations for several alkali halides with the NaCl structure equivalent to NiO.[32]

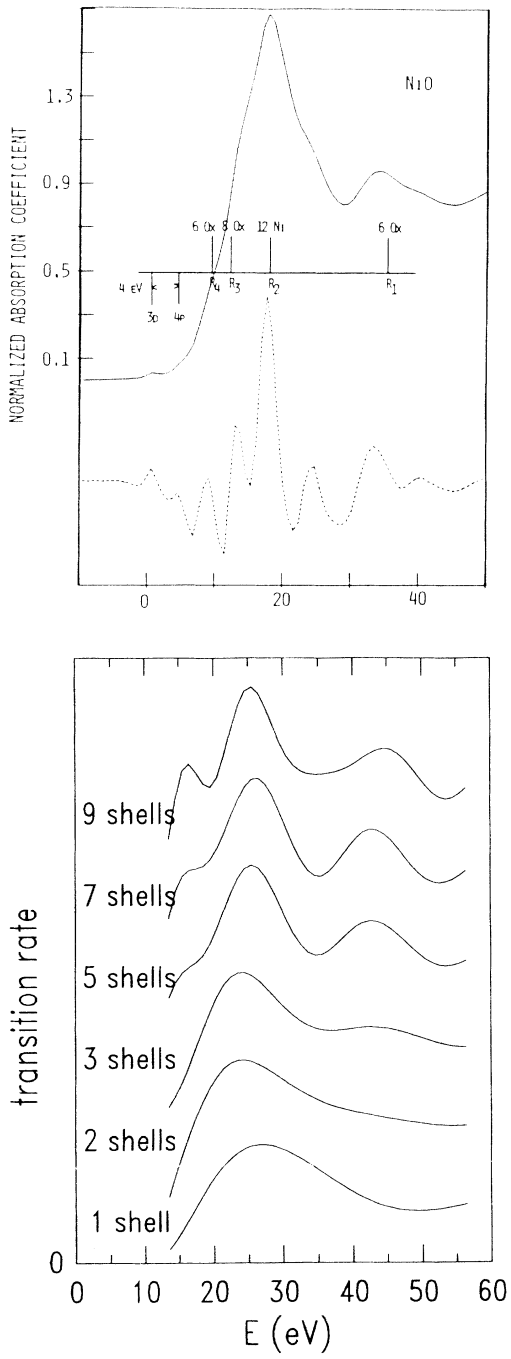

FIG. 2. Top: Experimental XANES data for NiO (Ref 12) together with the relationship between the XANES features and shells as suggested in Ref. 12. Bottom: Calculated XANES curves for NiO with different cluster sizes. For atomic distances and coordination numbers of the clusters see Table I. Calculations are performed with single scattering.

It is interesting to note that the introduction of an oxygen shell introduces more novelties into the spectrum than a Ni shell does: The third shell strongly enlarges the peak around 42 eV, the fifth shell causes the peak around 18 eV, and the eighth and ninth shells introduce the pronounced splitting of the main peak and the shoulder on its right-hand side around 28 eV. The same stands for calculations performed with only single-scattering calculations as shown in Fig. 2. This demonstrates the numerically different scattering power of the O^{2-} ions as compared to the Ni^{2+} ion and can also be named a "caging effect" of the O shell on the excited electron. In other words, the backscattering creates a relatively sharp quasibound scattering resonance around the absorber atom.[21]

The curved wave single-scattering results from Fig. 2, in comparison with the full multiple-scattering results of Fig. 1, demonstrate the impact of multiple scattering onto the final result. For the single-scattering calculations, the "$R=\lambda$" approximation of the phenomenological approach should instead be valid without being disturbed by multiple scattering. Nevertheless, the invalidity of correlating the first oxygen shell to the peak around 43 eV becomes even clearer. The numerical error introduced by the plane-wave approximation and the impact of the scattering phase shifts therefore cannot be neglected like it had been done in the approach of Ref. 12.

To elucidate the contribution of the single shells from another point of view, in Fig. 3, single-scattering XANES curves are displayed as calculated for single shells, without the closer inner shells. Results for the oxygen shells again are preferred for this figure because in this energy range oxygen atoms have a stronger electron scattering power, thus contribute more to the XANES spectrum. Again one can recognize manifold features in different energy ranges.

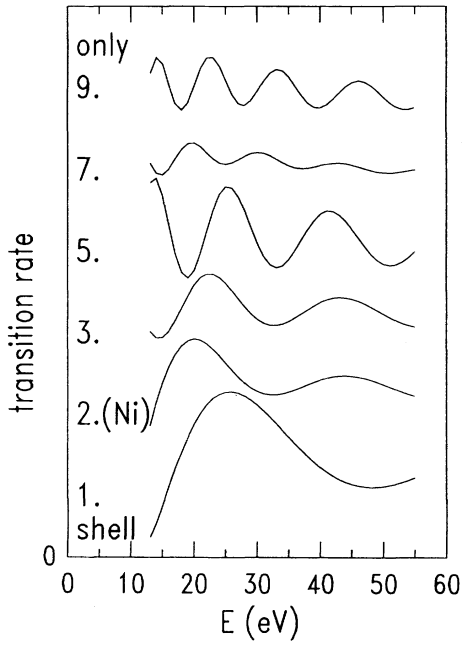

FIG. 3. Calculated XANES curve single shells selected from the NiO structure. Calculations are performed with single scattering.

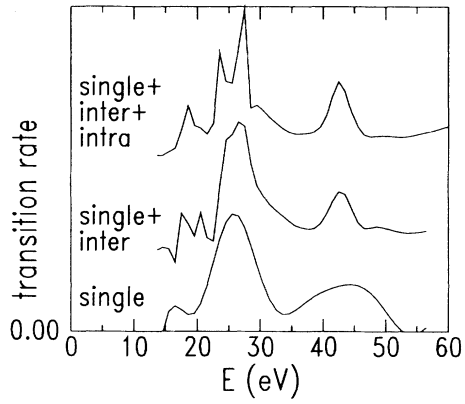

FIG. 4. Calculated XANES curves for NiO, cluster size: nine shells. Calculations are performed with full multiple plus single scattering (top line), only intershell multiple plus single scattering (middle line), and only single scattering (bottom line).

In Fig. 4, the results of the calculation for NiO with a cluster size of nine shells and with restrictions of scattering are displayed: bottom line: only single scattering; middle line: like the bottom line plus intershell multiple scattering, i.e., multiple scattering only in a linear direction, not on looped paths; and top line: like the foregoing calculation (middle line) plus intrashell multiple scattering, i.e., multiple scattering also on triangular or otherwise looped patterns.

It can be recognized that intershell multiple scattering plays the most important role to make the single-scattering result agree with the experimental data. The looped "intrashell" multiple-scattering paths do not add any extra structure to the result, they only make the features more pronounced.

B. Results for Cu

In Fig. 5 the calculation results for a Cu cluster of different sizes are displayed, again together with the corresponding Fig. 4 out of Ref. 12. For shell distances and coordination numbers see Table II. Again the electron damping term was chosen to be smaller than realistic, therefore, the peaks close to the edge are sharper than in the experimental data. The agreement between the experimental and calculated data is very good, both in amplitude and energy position, even for the weak bump at $E=17$ eV. Due to the position of the Fermi level, i.e., the edge position, the structure below 10 eV cannot be recognized in the experimental data.

In Fig. 6 the results for the plane-wave single-scattering case are displayed. It can be recognized that in this case the impact of multiple scattering on the result is much smaller than in the case of NiO. Above 30 eV it is not noticeable at all, it becomes apparent only below 30 eV. It has been argued previously[33] that curved wave single-scattering calculations can explain an XAFS curve down to the XANES range. A comparison of the results for NiO and Cu demonstrates that this statement cannot

be generalized. Its validity depends on the material and on the energy range under discussion. As for the NiO example, also the calculations for Cu demonstrate that the basis of the phenomenological approach has to be abandoned.

III. EXPERIMENTAL XANES DATA FOR Cu

Recently published experimental XAFS data[34] obtained from Cu layers down to monolayer thickness pro-

TABLE II. Shell distances and identities for Cu (fcc).

Shell No.	Element	N	r(nm)
1	Cu	12	0.255
2	Cu	6	0.361
3	Cu	24	0.442
4	Cu	12	0.510
5	Cu	24	0.571

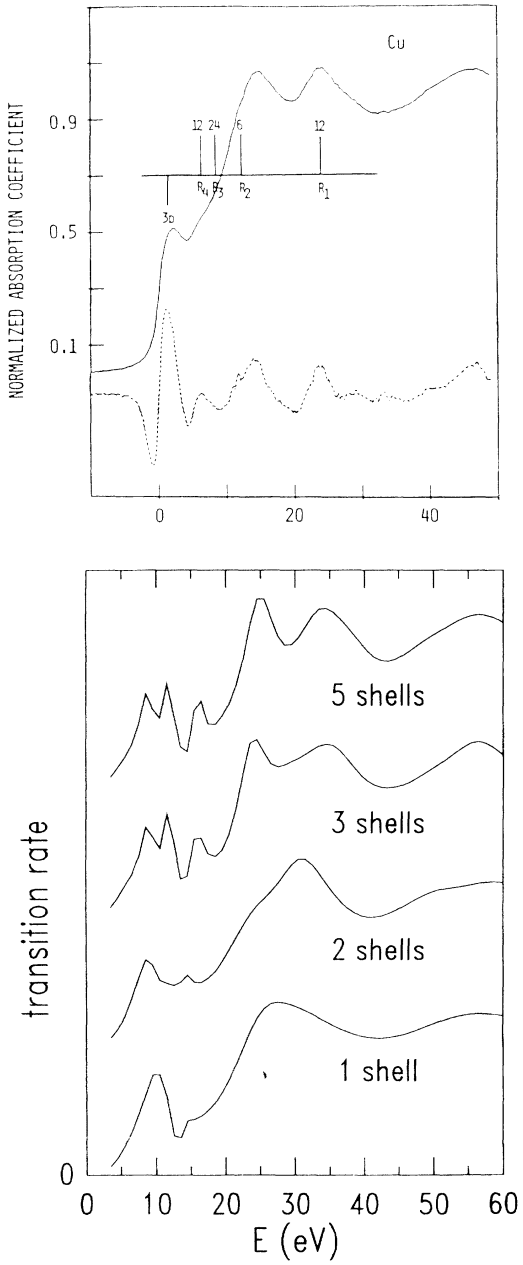

FIG. 5. Top: Experimental XANES data for Cu (Ref. 12) together with the relationship between the XANES features and shells as suggested in Ref. 12. Bottom: Calculated XANES curves for Cu with different cluster sizes. For atomic distances and coordination numbers of the clusters see Table II. Calculations are performed with full multiple scattering.

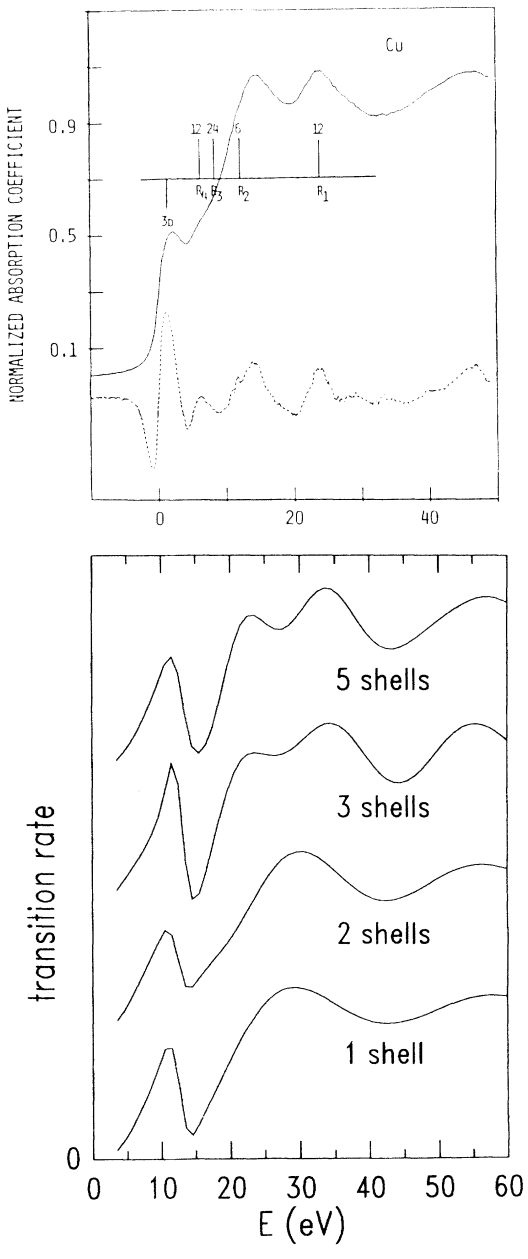

FIG. 6. Top: Experimental XANES data for Cu (Ref. 12) together with the relationship between the XANES features and shells as suggested in Ref. 12. Bottom: Calculated XANES curves for Cu with different cluster sizes. For atomic distances and coordination numbers of the clusters see Table II. Calculations are performed with single scattering.

vide a valuable analogy to the theoretical data from Sec. II B and from Ref. 21. The structure of the experimental XANES spectrum develops with an increasing number of shells similar to the theoretical calculations. However, unlike in the case of the calculations, the number of atomic layers necessary to develop the XANES spectrum completely is larger than the number of shells required to calculate the correct spectrum. This stems from the fact that, in the case of a smaller number of Cu layers, there is still a considerable disorder within the Cu bulk, which can also be monitored from the Fourier transform of the EXAFS data.[34] Secondly, due to the grazing incidence measurement geometry, a considerable fraction of probed Cu atoms is not covered with neighbor atoms from all sides, which also means a lack of medium-range order, which is necessary for the XANES. But the general trend of how an XANES spectrum evolves with increasing medium-range order is reproduced and confirms the theoretical calculations.

IV. VALIDITY OF THE PHENOMENOLOGICAL APPROACH FOR SINGLE SHELLS

Although the phenomenological approach has been disproved for bulk materials, there is still the possibility to apply it for cases with single shells. The general relationship between the atomic distances and a contraction of the XANES energy scale is an established fact, both by experimental studies (see, e.g., Ref. 11) and by theoretical calculations, e.g., for the Fe-K edge in the $K_3Fe(CN)_6$ molecule[35] or in the crystalline Fe_2B alloy.[3]

But even for the case of a single shell, the multiple-scattering effect shifts the energy positions of the XANES peaks away from the energy positions of the single-scattering peaks, which form the basis for the simplified approach. The amount of this shift can neither be generalized nor predicted, see, e.g., all single-shell results in Figs. 1–5. More examples of the difference between single- and multiple-scattering results can be found in Refs. 3, 20, and 36–38.

Therefore, it seems that the phenomenological approach can only be applied to a comparison among single-shell compounds with the same geometry, i.e., the same amount of interference from multiple scattering.

V. CONCLUSION

XANES spectra have been calculated with a full multiple-scattering computer code for two materials which had been used as prototypes for a simplified XANES data evaluation scheme. Detailed calculations together with recently published experimental data show that, due to the complexity of the scattering processes, the fundamental aspect of this scheme is questionable as well as its application. For XANES investigations of solids there is no way to avoid sophisticated multiple-scattering or density-of-states calculations.

ACKNOWLEDGMENT

F. W. Lytle's deep interest in this paper, his helpful discussions, and his provision of the original drawings used for Ref. 12 are gratefully appreciated.

[1]Proceedings of the Workshop of Investigations of Higher Order Correlation Functions "Beyond Radial Distribution," Grenoble, France, edited by J. B. Suck, D.Quitmann, and B. Maier [J. Phys. (Paris) Colloq. **46**, C9-1 (1985)].

[2]P. J. Durham, J. B. Pendry, and C. H. Hodges, Solid State Commun. **38**, 159 (1981).

[3]P. Kizler, P. Lamparter, and S. Steeb, in Proceedings of the 5th XAFS-Conference Seattle, WA 1988, edited by J. M. de León, E. A. Stern, D. E. Sayers, Y. Ma, and J. J. Rehr [Physica B **158**, 392 (1989)].

[4]J. Petiau, G. Calas, and P. Sainctavit, in Proceedings of the International Conference on X-ray and Inner-Shell Process, Paris, France, 1987 [J. Phys. (Paris) Colloq. **48**, C9-1085 (1987)]; D. D. Vvedensky, in *Unoccupied Electronic States: Fundamentals for XANES, EELS, IPS and BIS,* edited by J. C. Fuggle and J. E. Inglesfield (Springer, Berlin, 1992).

[5]Examples can be found in Ref. 4 as well as in all proceedings of the conferences on x-ray-absorption fine structure.

[6]F. Sette, J. Stöhr, and A. P. Hitchcock, Chem. Phys. Lett. **110**, 517 (1984).

[7]J. Stöhr, F. Sette, and A. L. Johnson, Phys. Rev. Lett. **53**, 1684 (1984).

[8]A. P. Hitchcock, F. Sette, and J. Stöhr, in Proceedings of the 3rd EXAFS Conference, Stanford, CA 1984, edited by K. O. Hodgson, B. Hedman, and J. E. Penner-Hahn (Springer, Berlin, 1984), p. 43.

[9]C. R. Natoli, in Proceedings of the 1st EXAFS Conferences Frascati, Italy, edited by A. Bianconi, L. Incoccia, and S. Stipcich (Springer, Berlin, 1983), pp. 43 and 57; C. R. Natoli, in Proceedings of the 3rd EXAFS Conference, Stanford, CA, 1984, edited by K. O. Hodgson, B. Hedman, and J. E. Penner-Hahn (Springer, Berlin, 1984) p. 38.

[10]M. Benfatto, C. R. Natoli, J. Garcia, and A. Bianconi, in Proceedings of the 4th EXAFS Conference Fontevraud, France, 1986, edited by P. Lagarde, D. Raoux, and J. Petiau [J. Phys. (Paris) Colloq. **47**, C825 (1986)].

[11]A. Bianconi, E. Fritsch, G. Calas, and J. Petiau, Phys. Rev. B **32**, 4929 (1985).

[12]F. W. Lytle, R. B. Greegor, and A. J. Panson, Phys. Rev. B **37**, 1550 (1988).

[13]P. Mahto and A. R. Chetal, in Proceedings of the 5th XAFS Conference, Seattle, WA, edited by J. M. de Léon, E. A. Stern, D. E. Sayers, Y. Ma, and J. J. Rehr [Physica B **158**, 415 (1989)].

[14]M. Kasrai, M. E. Fleet, G. M. Bancroft, K. H. Tan, and J. M. Chen, Phys. Rev. B **43**, 1763 (1991).

[15]M. Kasrai, J. D. Bozek, L. L. Coatsworth, M. E. Fleet, T. K. Sham, K. H. Tan, J. R. Brown, and G. M. Bancroft, in Proceedings of the 5th XAFS Conference, Seattle, WA, 1988, edited by J. M. de Léon, E. A. Stern, D. E. Sayers, Y. Ma, and J. J. Rehr [Physica B **158**, 515 (1989)].

[16]M. Kasrai, G. M. Bancroft, D. G. Sutherland, M. E. Fleet, K.

H. Tan, and J. M. Chen, in Proceedings of the 6th XAFS Conference, York, UK, 1990, edited by S. Hasnain (Horwood, Chichester, UK 1991), p. 601.

[17]F. W. Lytle, Ber. Bunsenges. Phys. Chem. **91**, 1251 (1986).

[18]K. B. Garg, K. Jerath, H. S. Chauhan, and U. Chandra, Pramana J. Phys. **27**, 821 (1986).

[19]A. K. Chakraborty, A. R. Chetal, and P. R. Sarode, Phys. Status Solidi A **130**, 19 (1992).

[20]D. Norman, K. B. Garg, and P. J. Durham, Solid State Commun. **56**, 895 (1985).

[21]T. Lindner, H. Sauer, W. Engel, and K. Kambe, Phys. Rev. B **33**, 22 (1986).

[22]G. N. Greaves, P. J. Durham, G. Diakun, and P. Quinn, Nature **294**, 139 (1981).

[23]D. D. Vvedensky, D. K. Saldin, and J. B. Pendry, Comput. Phys. Commun. **40**, 421 (1986).

[24]J. B. Pendry, *Low Energy Electron Diffraction* (Academic, London, 1974); T. L. Loucks, *The Augmented Plane Wave Method* (Benjamin, New York, 1967).

[25]E. Clementi and C. Roetti, At. Data. Nucl. Data Tables **14**, 177 (1974).

[26]P. J. Durham, J. B. Pendry, and C. H. Hodges, Comput. Phys. Commun. **25**, 193 (1982).

[27]D. D. Vvedensky and J. B. Pendry, Surf. Sci. **152/153**, 33 (1985).

[28]B. K. Teo, *EXAFS: Basic Principles and Data Analysis* (Springer, Berlin, 1986), Chap. 5.2; M. P. Seah and W. A. Dench, Surf. Inter. Anal. **1**, 2 (1979).

[29]J. Garcia, A. Bianconi, M. Benfatto, and C. R. Natoli, in Proceedings of the 4th EXAFS Conference, Fontevraud, France, edited by P. Lagarde, D. Raoux, and J. Petiau [J. Phys. (Paris) Colloq. **47**, C8-51 (1986)].

[30]P. A. Lee and G. Beni, Phys. Rev. B **15**, 2862 (1977).

[31]S. T. Pantelides, D. J. Mickish, and A. B. Kunz, Phys. Rev. B **10**, 5203 (1974).

[32]L. A. Bugaev, I. I. Gegusin, A. A. Novakovich, and R. V. Vedrinskii, in Proceedings of the 4th EXAFS Conference, Fontevraud, France, 1986, edited by P. Lagarde, D. Raoux, and J. Petiau [J. Phys. (Paris) Collog. **47**, C8-101 (1986)]; L. A. Bugaev and R. V. Vedrinskii, Phys. Status Solidi B **132**, 459 (1985); **151**, 581 (1989).

[33]S. J. Gurman, N. Binsted, and I. Ross, J. Phys. C **17**, 143 (1984); **19**, 1845 (1986); J. E. Müller and W. Schaich, Phys. Rev. B **27**, 6489 (1983).

[34]R. Frahm, T. W. Barbee, and W. Warburton, Phys. Rev. B **44**, 2822 (1991).

[35]A. Bianconi, M. Dell'Ariccia, P. J. Durham, and J. B. Pendry, Phys. Rev. B **26**, 6502 (1982).

[36]P. Kizler, P. Lamparter, and S. Steeb, Z. Naturforsch. Teil A **44**, 7 (1989); **44**, 189 (1989).

[37]D. D. Vvedensky and J. B. Pendry, Surf. Sci. **162**, 903 (1985).

[38]C. E. Bouldin, D. A. McKeown, R. A. Forman, J. J. Ritter, and G. Bunker, Phys. Rev. B **38**, 10 816 (1988).